Biochimie 194 (2022) 118–126

Contents lists available at ScienceDirect

Biochimie

journal homepage: www.elsevier.com/locate/biochi

Function and versatile location of Met-rich inserts in blue oxidases involved in bacterial copper resistance

Frédéric Roulling, Amandine Godin, Georges Feller*

Laboratory of Biochemistry, Center for Protein Engineering - InBioS, University of Liège, Belgium

ARTICLE INFO

Article history:
Received 11 August 2021
Received in revised form
7 December 2021
Accepted 29 December 2021
Available online 1 January 2022

Keywords:
Multicopper oxidase
Cuproxidases
CueO
Copper resistance
Laccase
Extremophiles

ABSTRACT

Cuproxidases form a subgroup of the blue multicopper oxidase family. They display disordered methionine-rich loops, not observable in most available crystal structures, which have been suggested to bind toxic Cu(I) ions before oxidation into less harmful Cu(II) by the core enzyme. We found that the location of the Met-rich regions is highly variable in bacterial cuproxidases, but always inserted in solvent exposed surface loops, at close proximity of the conserved T1 copper binding site. We took advantage of the large differences in loop length between cold-adapted, mesophilic and thermophilic oxidase homologs to unravel the function of the methionine-rich regions involved in copper detoxification. Using a newly developed anaerobic assay for cuprous ions, it is shown that the number of Cu(I) bound is nearly proportional to the loop lengths in these cuproxidases and to the number of potential Cu(I) ligands in these loops. In order to substantiate this relation, the longest loop in the cold-adapted oxidase was deleted, lowering bound extra Cu(I) from 9 in the wild-type enzyme to 2–3 Cu(I) in deletion mutants. These results demonstrate that methionine-rich loops behave as molecular octopus scavenging toxic cuprous ions in the periplasm and that these regions are essential components of bacterial copper resistance.

1. Introduction

Since the advent of dioxygen produced by cyanobacteria about 10^9 years ago, copper has become an essential element for most living organisms. Indeed, oxidation of water-insoluble Cu(I), mainly in the form of sulfides, has provided soluble and more bioavailable Cu(II), which was ideally suited to exploit the oxidizing power of dioxygen [1,2]. The redox properties of the Cu(I)/Cu(II) couple make it an invaluable cofactor in proteins for electronic transfer process or redox transformation but are also responsible for severe hazards to the cell, for example by generating highly toxic hydroxyl radical in a Fenton-like reaction [3]. Moreover, copper can bind non-specifically to proteins or replace other metallic cofactors therefore impairing protein function [4,5]. Organisms have evolved several systems to finely control cellular copper levels and to resist to elevated concentrations in their environment mainly by the use of pumps and metallochaperones [2]. One of them, the Cue system (Cu efflux) was first discovered in *Escherichia coli* and, with the high number of genome sequences now available, it is considered widespread in aerobic Gram-negative bacteria [6]. This system consists of a copper responsive element, CueR, that can activate the expression of CopA, a transmembrane P-type ATPase which pumps Cu(I) from the cytoplasm into the periplasm, and of CueO (Cu efflux oxidase), a periplasmic multicopper oxidase which converts Cu(I) into the less toxic Cu(II) [7].

Multicopper oxidases (MCOs) are blue enzymes that catalyze the one-electron oxidation of various substrates and the concomitant four-electron reduction of dioxygen to water, the latter activity being only shared with terminal oxidases [8]. Their mechanism of action is based on an active site of four copper ions classified into three main copper spectroscopic types (Figs. 1 and 2). Substrates bind near the T1 site, responsible for the blue color, which transfers electrons to the trinuclear center (TNC), unique to MCOs and formed by a binuclear T3 site and a T2 copper, where oxygen is reduced to water [8]. Metallo-oxidases are a subset of the

Abbreviations: CueO, cuproxidase from *E. coli*; *Tth*-MCO, cuproxidase from the thermophile *Thermus thermophilus*; *Pha*MOx, cuproxidase from the psychrophile *Pseudoalteromonas haloplanktis*; DSC, differential scanning calorimetry.

* Corresponding author. Laboratory of Biochemistry, Institute of Chemistry B6a, B-4000, Liège-Sart Tilman, Belgium.
E-mail address: gfeller@uliege.be (G. Feller).

https://doi.org/10.1016/j.biochi.2021.12.015
0300-9084/

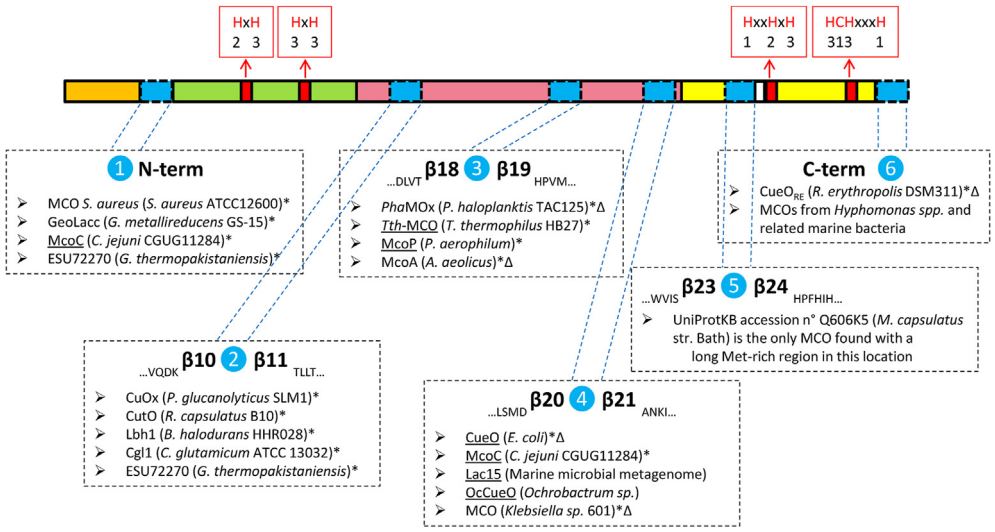

Fig. 1. Primary structure organization in cuproxidases. The six possible locations (in blue) for insertion of Met-rich loops depicted in a schematic view of CueO primary structure. Signal peptide in orange. Cupredoxin domains 1, 2 and 3 in green, pink and yellow, respectively. The four ultra-conserved catalytic copper binding sites are located in red. Red boxes indicate the copper chelating residues in red and the numbers refer to the spectroscopic copper types. The sequence directly preceding the third conserved catalytic copper binding site and consisting of D and/or M and/or H residues specific to cuproxidases and forming the inner part of the sCu binding site is in white. Blue boxes and numbers in blue circles indicate the six loop locations where a Met-rich region can be found in different cuproxidases. The numbering of β-sheets is based on CueO structure 3OD3 and the four residues of each extremity of β-sheets in CueO framing the insertion loops are indicated in subscript for clarity (see Figs. S1 and S2). Selected examples of cuproxidases are indicated for each location. The asterisk * indicates that this MCO has been characterized and at least one publication is available. The delta symbol Δ indicates that a mutant where the Met-rich region has been (partially) deleted or mutated was constructed and characterized. The six cuproxidases for which a crystal structure is available are underlined.

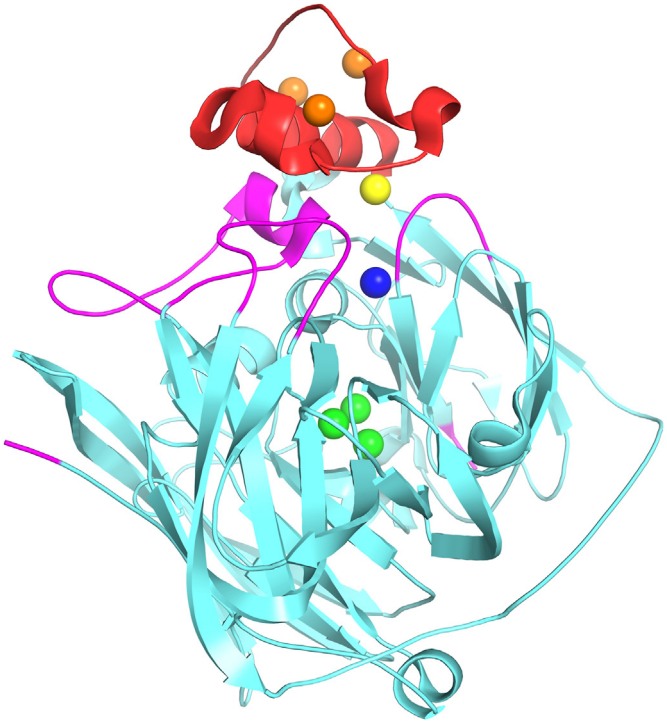

Fig. 2. Ribbon diagram of CueO from *E. coli*. In red, the Met-rich insert in CueO and in magenta, the solvent-exposed loops in which the Met-rich insert has been found in other bacterial cuproxidases. Note the proximity with the blue T1 site. Spheres represent bound copper ions with color code: blue, the T1 Cu; green, the trinuclear center; yellow, the sCu and orange, Cu(I) on the Met-rich region. The N-terminus (magenta) is in front, left and the C-terminus (magenta) is behind the structure. Figure based on PDB entries 3OD3 and 3NT0.

MCO family in which substrates are low-valent first-row transition metal ions such as Fe(II), Cu(I) and/or Mn(II) [9–11]. This subset includes cuproxidases (cuprous oxidases) and the well-studied ferroxidases (ferrous oxidases) Fet3p from yeast and human ceruloplasmin that illustrate the biological connection of copper to iron, making the former metal mandatory to aerobic metabolism of the latter in eukaryotes [12].

The structure of CueO (the cuproxidase from *E. coli*) displays the general fold of MCOs, consisting of three repeated beta-stranded cupredoxin domains, with an additional methionine-rich (Met-rich) region (Fig. 2) that restricts accessibility to the T1 site and confers specificity for Cu(I) [13]. This striking feature contrasts with other MCOs such as laccase or ascorbate oxidase where a depression near the T1 site creates a substrate specific site for phenolic compounds or ascorbic acid, respectively [14]. Met-rich regions are associated with several proteins involved in copper management and homeostasis, notably the high affinity copper transporters (Ctr) widely conserved from yeast to human. Recent structural and functional analysis of CueO showed that its Met-rich region provides additional Cu(I) binding sites, one of which is the sCu site (s standing for substrate). According to the reaction mechanism proposed for CueO, Cu(I) ions are gathered via the methionine-rich region, mainly a disordered loop, and the adjacent substrate binding site (sCu). The latter is buried underneath the protein surface and H-bonded to the T1 site, suggesting an electron transfer pathway from sCu to the T1 site and then to the TNC where oxygen is reduced to water [8,14,15]. The Cu(I) binding sites in the Met-rich region have been described as substrate-docking-oxidation sites, whereas the sCu site connects surface-exposed sites to the catalytic T1 site [15]. However, both the length and composition of the Met-rich insert are highly variable in other bacterial cuproxidases [16,17] but this aspect has not been investigated so far.

We report here the characterization of blue multicopper oxidases produced by bacteria living in different temperature niches. To conduct investigations on the function of Met-rich regions in bacterial MCOs, three model enzymes were chosen: CueO from the mesophilic bacterium *Escherichia coli* [13] because this enzyme has been extensively studied and its 3D-structure determined [14,18],

the thermophilic *Tth*-MCO, the corresponding MCO from *Thermus thermophilus* HB27 [19,20] and *Pha*MOx, a new psychrophilic (cold-adapted) MCO encoded in the genome of the Antarctic bacterium *Pseudoalteromonas haloplanktis* TAC125 [21,22]. The three enzymes are homologous periplasmic cuproxidases with laccase-like activity. Taking advantage of the large loop length differences in extremophilic cuproxidases and by mutagenesis of *Pha*MOx, we show here that the number of Cu(I) bound is nearly proportional to the size of the Met-rich loops and to the number of potential Cu(I) ligands (Met, His, Asp) and propose that these flexible loops behave as molecular octopus, scavenging toxic cuprous ions in the periplasm.

2. Materials and methods

2.1. Construction of expression plasmids and mutagenesis

Genomic DNA was extracted from a batch culture of *P. haloplanktis* TAC125 or *E. coli* JM109 using the Promega wizard genomic DNA purification kit. The coding sequences were PCR-amplified using $Vent_R$ Thermopol Polymerase (New England Biolabs), with the forward primers containing a *Nco*I site and the reverse primers containing a *Xho*I site and the stop codon (Table S1). The PCR products were cloned into the pSP73 cloning vector (Stratagene), excised with *Nco*I and *Xho*I and ligated into the pET28a (+) vector (Novagen). Mutants of *Pha*MOx were obtained using inverse PCR with the pET28a plasmid harboring the *Pha*MOx coding sequence as template and primers listed in Table S1. The resulting recombinant plasmids were transformed into *E. coli* BL21 (DE3) cells (Stratagene). Plasmid pTL1 harboring the *Tth*-MCO coding sequence was obtained as previously described [19].

2.2. Production and purification of recombinant PhaMOx, CueO, Tth-MCO and mutants of PhaMOx

Single colonies of *E. coli* BL21 (DE3) cells transformed with the pET28a vector carrying the MCO gene were used to inoculate a 30 ml preculture in LB containing 50 μg ml^{-1} kanamycin at 37 °C. This preculture was used to inoculate 330 ml of Terrific broth (12 g l^{-1} Bacto tryptone (Difco), 24 g l^{-1} yeast extract (Difco), 4 ml l^{-1} glycerol, 12.54 g l^{-1} K_2HPO_4, 2.31 g l^{-1} KH_2PO_4, pH 7.2) containing 50 μg ml^{-1} kanamycin in 2-L flasks. The cultures were incubated at 37 °C and 250 rpm until an absorbance at 600 nm reached about 5. Expression of the enzymes was induced with 0.1 mM isopropyl-1-thio-β-galactopyranoside. Following a further 20-h incubation at 18 °C, the cells were harvested by centrifugation at 10,000×*g* for 30 min at 4 °C, resuspended in 50 mM Tris, pH 8.0 supplemented with protease inhibitors (Complete EDTA-free, Roche) and disrupted in a prechilled high-pressure cell disrupter (EmulsiFlex-C3, Avestin). Cell debris were removed by centrifugation at 40,000×*g* for 30 min at 4 °C. Supernatants were supplemented with Benzonase and $MgCl_2$ and dialyzed overnight against 50 mM Tris, 1 mM $CuSO_4$, 1 mM PMSF, pH 8.0. The dialysate, which had turned blue, was then loaded on a Q-Sepharose Fast Flow (GE Healthcare) column equilibrated in 50 mM Tris, 1 mM PMSF, pH 8.0 and eluted using a linear gradient from 0 to 300 mM NaCl in the buffer. Active fractions were pooled and dialyzed against 50 mM acetate, 1 mM PMSF, pH 5.0. After centrifugation, the sample was loaded on a S-Sepharose Fast Flow (GE Healthcare) column equilibrated in the same buffer and eluted with a linear gradient (0–300 mM NaCl). Active fractions were dialyzed against 10 mM K_2HPO_4, 1 mM PMSF, pH 7.0 and further purified on a Hydroxyapatite column (Bio-Rad) using a linear gradient from 10 to 300 mM K_2HPO_4. Active fractions were pooled, dialyzed against 50 mM Tris, pH 8.0 and concentrated using an Amicon ultrafiltration device with a 10 kDa cut-off membrane (Millipore). CueO was purified as described [36], except that all steps were carried out at 4 °C and *Tth*-MCO was purified as previously described [19]. Protein concentration was determined by the Bradford assay using bovine serum albumin as a standard.

2.3. Copper loading

All enzymes preparations were loaded with a 15-fold excess of Cu(I) and excess was removed with PD10 columns (Amersham). Cu(I) was added from a 20 mM stock solution of $[Cu(I)(MeCN)_4]PF_6$ complex in acetonitrile. Holoenzymes were used in all experiments, except differential scanning calorimetry (see below). Copper content of enzymes samples was determined by the 2,2′-biquinoline method [32]. Hydroxylamine was added in the detection reagent for the determination of total copper, while it was omitted for the determination of copper present as cuprous state in the sample, referred to as “Cu total” and “Cu(I)”, respectively, in the measurements results.

2.4. Copper binding assay

Cu(I) binding capacity of the holoenzymes was determined in a similar manner as for the preparation of the holoenzymes but in fully anaerobic conditions. The experiment was carried out under N_2 atmosphere in an inflatable glove bag (Cole-Parmer). Aqueous solutions were degassed by bubbling with N_2 gas overnight prior transfer to the inflatable glove bag. Holoenzymes were diluted at 15 μM in 50 mM Tris, pH 8 and Cu(I) was added at a final concentration of 225 μM from a 20 mM stock solution of $[Cu(I)(MeCN)_4]PF_6$ complex in acetonitrile. The enzyme solution was incubated for 1 min and then applied to a PD10 column previously equilibrated in freshly prepared 50 mM Tris, 5 mM ascorbic acid, pH 8. Ascorbic acid was added in the degassed buffer solution just prior use from a freshly prepared 500 mM stock solution made inside the glove bag using degassed water. The column was directly eluted with the same strongly-reducing buffer and the elution was collected in several fractions in order to separate the late-eluting protein-containing fractions from the early-eluting excess-copper-containing fractions. Protein-containing fractions were then directly subjected to copper content determination.

2.5. Analytical procedures

N-terminal amino acid sequence of the recombinant enzymes was determined by automated Edman degradation using a pulsed-liquid-phase protein sequencer Procise 494 (Applied Biosystems). Mass determination was performed on an ESI-Q-TOF instrument (Waters, Micromass) in positive ion mode. Samples (10 μM) were analyzed in 30% acetonitrile, 0.5% formic acid, 25 mM ammonium acetate. Spectra deconvolution technique of calculation was the maximum entropy (Max ent1). Circular dichroism spectra of the holoenzymes were recorded using a Jasco J-810 spectropolarimeter under constant nitrogen flow. Spectra in the far UV were recorded at 20 °C in a 0.1 cm quartz cell at a protein concentration of ~100 μg ml^{-1} in 50 mM Tris, pH 7.5. For near UV spectra, 1 mg ml^{-1} concentration and 1 cm optical path length were used. Spectra were averaged over five scans and corrected for the buffer signal. Differential scanning calorimetry experiments carried out with apoenzymes and laccase-like activity tests using 2,6-dimethoxyphenol as substrate were performed as described previously [22].

3. Results

3.1. Location of the Met-rich region in bacterial cuproxidases

In order to compare the three investigated cuproxidases *Pha*-MOx, CueO and *Tth*-MCO with previously characterized bacterial homologs, a search was performed in the literature for MCOs displaying a Met-rich region, or involved in copper resistance, or experimentally confirmed as having a cuproxidase activity. This subset of 34 homologs included 6 cuproxidases for which a 3D structure has been solved (Table S2). They belong to both Gram negative and positive bacteria and are mainly secreted via the Tat (Twin-arginine translocation) export machinery specialized in the transport of folded and cofactor-containing proteins across the cytoplasmic membrane of prokaryotes [23]. However, some are Sec-dependently translocated according to the SignalP-5.0 analysis (Table S2) and as already reported [24]. The multiple sequence alignment of these homologs (Fig. S1) combined with the structural alignment of the 6 crystal structures (Fig. S2) allowed to locate the Met-rich regions within the secondary structures. The most interesting result was the position of the Met-rich region in these bacterial MCOs, which is highly variable in the sequence and frequently differs from the canonical position in CueO. In total, 5 different Met-rich region locations were identified (Fig. 1). To further reinforce this result, additional BLAST searches were performed with the purpose of exploring the vast amount of bacterial MCOs sequences available, particularly those displaying a long Met-rich region in their primary structure. Consequently, a new sequence alignment made of the 34 MCOs enriched with a selection of additional sequences discovered from the BLAST searches allowed to confirm the different possible locations - and also to highlight the variable amino acid composition - of the Met-rich region in 93 homologs (Fig. S3). Interestingly, a sixth Met-rich region location was found in this alignment, but in a single MCO sequence from the obligate methanotroph *Methylococcus capsulatus* str. Bath (Fig. S3). As shown in Fig. 2, based on crystal structures of CueO, the identified Met-rich regions are inserted at positions corresponding to 6 different solvent exposed surface loops in CueO, 4 framed by beta-sheets, and 2 as tails at the N-terminus and at the C-terminus, all being located at close proximity of the strictly conserved T1 copper binding site. In contrast to CueO depicted in Fig. 2, the long N-terminus loop of McoC, which contains the Met-rich region, extends toward the T1 site in the crystal structure [25]. In *R. erythropolis* and various actinobacteria, the Met-rich region is a C-terminal tail which was modelled and was found to point towards the T1 site [26].

Several MCOs possess two Met-rich-regions, such as in McoC [25] with one at the N-terminus and one in the Met-rich region 4. Various MCO sequences from marine bacteria (*Hyphomonas* spp., *Hirschia maritima*, *Henriciella marina*, *Oceanicaulis alexandrii*, *Maricaulis maris*) were found to have a long C-terminal Met-rich region, but also a long Met-rich region in position 3 or 4 (Fig. S3). A common observation on the Met-rich inserts was that they are composed by a conserved or semi-conserved motif repeated several times. As an example, the Met-rich region of *S. aureus* P0218 is formed by 5 repeats of the motif MMDMK separated by semi-conserved residues. The Met-rich regions found in CueO, *Tth*-MCO, *Pha*MOx and some cuproxidases are flanked by an N-terminal M(X)DM(X)G sequence (with X standing for any residue or none), forming the solvent-exposed outer part of the sCu site in CueO [27] and a D(X) (X)MX sequence immediately upstream from the motif consisting of the three strictly conserved copper-binding histidines, forming the buried inner part of the sCu site (Fig. S4). The size of the Met-rich region is also highly variable, ranging from its absence with only the sCu sequences like for *M. tuberculosis* MCO (Table S2) to about 130 residues, for instance in *P. putida* MCO Pp-CopA (Fig. S1). The size of the Met-rich region is apparently not related to temperature adaptation in contrast to what is frequently reported for non-functional loops in extremophiles [28]. For instance, the cuproxidase *Pha*MOx from the Antarctic *P. haloplanktis* displays a long 55 residue insert whereas both cuproxidases from the Arctic *Psychrobacter arcticus* 273-4 and *Psychrobacter cryohalolentis* K5 from Siberian permafrost are devoid of the Met-rich region and only display both conserved motifs of the sCu site in their cuproxidases (Fig. S5), although the three enzymes share 55% identity (82% similarity) in the core enzyme. Finally, the occurrence of a cuproxidase in bacteria is unpredictable: whereas the investigated *Tth*-MCO was isolated from *T. thermophilus* HB27, the genome of *T. thermophilus* HB8 is devoid of a cuproxidase coding sequence.

3.2. Genomic context and primary structure of the investigated blue oxidases

The multicopper oxidase *Pha*MOx encoded by the PSHAb0011 gene in the genome of the Antarctic bacterium *Pseudoalteromonas haloplanktis* TAC125 [21] is homologous to the cuproxidases CueO from the mesophile *E. coli* and to *Tth*-MCO from the thermophile *T. thermophilus* HB27. Like its two counterparts and despite genome annotation as a “putative laccase” [29], the function of the psychrophilic enzyme is clearly linked to copper resistance of the bacterium. Indeed, in the three bacteria, the gene encoding the MCO belongs to an operon also comprising a copper-responsive factor and a copper efflux P-type ATPase. General information on the investigated MCO is provided in Table 1. The three enzymes possess four ultra-conserved copper binding motifs typical of the MCO family and the Met-rich region specific to cuproxidases (Fig. 1, Fig. S4). They also display a signal peptide for periplasmic targeting by the Tat export pathway. The Met-rich regions specific to the cuproxidase sub-family are also very different in length and composition among the three MCOs and, with the regions surrounding them, are responsible for the differences in polypeptide size (Tables 1 and 2). In CueO, the Met-rich region is inserted at location 4, whereas the insertion is in location 3 for both *Tth*-MCO (Fig. 1) and *Pha*MOx, although for the latter insertion at location 4 cannot be ruled out (Fig. S1). In contrast to CueO and *Tth*-MCO, the 3D structure of *Pha*MOx is not known and its Met-rich insert has been delineated using the outer sCu consensus sequence and the Met and His abundance.

3.3. Cloning and production of the psychrophilic blue oxidase and of its homologs

The full-length coding sequence of the psychrophilic oxidase was cloned in a pET vector and expressed in *E. coli* BL21 (DE3). Laccase-like activity of the heterologously expressed enzyme was detected in the cytoplasmic fraction and to a much lower extent in the periplasmic fraction (data not shown). N-terminal sequencing of the new protein band observed by SDS-PAGE of the periplasmic fraction of induced cells confirmed both its identity and the cleavage site predicted by the SignalP server [30]. The heterologous Tat-signal is therefore recognized by the *E. coli* export machinery but the latter is apparently overloaded by the huge amounts of enzyme produced (estimated to ~0.5 g l^{-1} of culture). Indeed, most of the enzyme production was not processed and remained in the cytoplasm where different proteolytic cleavages occurred, leading to N-terminal heterogeneity in the Tat-signal peptide as deduced from N-terminal sequencing. Consequently, only the nucleotide sequence of the gene encoding the enzyme mature region was inserted in a pET vector and expressed. Purification of the recombinant psychrophilic mature enzyme *Pha*MOx was achieved by a

Table 1
General properties of the investigated multicopper oxidases.

Oxidase	Source	T_{env}[a] °C	TAT peptide aa	mature form aa	Mw kDa	UniProtKB acc n°
Tth-MCO	*T. thermophilus* HB27	~80	21	440	48.8	Q72HW2
CueO	*E. coli* JM109	37	28	488	53.4	P36649
*Pha*MOx	*P. haloplanktis* TAC 125	<0	36	576	64.2	Q3ICN9

[a] Estimated average environmental temperature.

Table 2
Properties of the Met-rich insert in the homologous blue oxidases.

Oxidase	Length aa	Met	His	Asp	∑ ligands
Tth-MCO	16	6	1	1	8
CueO	45	14	5	4	23
*Pha*MOx	55	14	7	8	29

combination of ion-exchangers. Both the Tat-processed (periplasmic) and the cytoplasmic-produced oxidases were found identical in terms of activity and stability. Accordingly, similar gene cloning and cytoplasmic production strategies were applied for CueO and *Tth*-MCO. Integrity of the purified proteins was confirmed by automated Edman N-terminal sequencing and ESI-Q-TOF mass spectrometry. The three recombinant MCOs appeared homogenous on SDS-PAGE and displayed laccase and ferroxidase activities (Fig. S6).

3.4. Circular dichroism spectra

As expected for MCOs formed by three cupredoxin domains, circular dichroism spectra in the far UV of holoenzymes showed that the secondary structures of the three cuproxidases essentially consist of beta-sheets (Fig. 3A). No alteration of these spectra were observed following addition of $CuSO_4$ or of the reducing agent hydroxylamine, showing that the copper redox state does not induce detectable secondary structure variations. CD spectra in the visible region displayed signals typical to T1 and T3 copper binding sites but clear differences were noted (Fig. 3B). As amino acids forming the copper binding motifs are strictly conserved among the three cuproxidases, these discrepancies should arise from slight differences in the lengths and angles between the bound copper and nitrogen or sulfur atoms from histidine or cysteine/methionine residues, respectively. In both UV regions, the CD spectra of the cold-adapted and thermophilic oxidases were similar and differed from the mesophilic CueO. Interestingly, this similarity pattern was also observed when comparing the flexibility of the 3 enzymes [22].

3.5. Copper binding by the homologous blue oxidases

The three cuproxidases were produced without supplemented copper ions in the culture medium in order to avoid induction of the endogenous chromosome-borne, copper-inducible cuproxidase of *E. coli* BL21 (DE3) and to increase the growth yield. The three purified enzymes displayed a blue color typical of MCOs but were not fully loaded with their cofactors. Indeed, addition of Cu(II) led to a very slow increase in color intensity, whereas addition of Cu(I) rendered the preparations instantly colorless due to reduction of the T1 copper and then rapidly more blue with increased absorbance at ~600 nm (T1 copper site) but also at ~340 nm (T3 copper site) (Fig. S7C). It has been shown that many apo-MCOs can only be completely loaded with copper in its cuprous Cu(I) and not cupric Cu(II) state [31] as Cu(I) is more exchange labile and is the

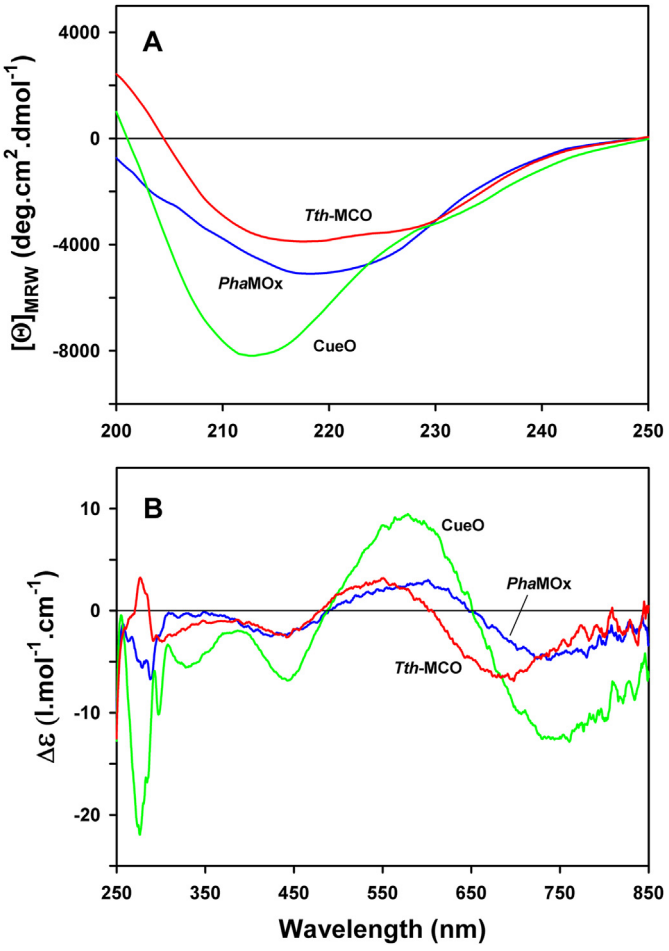

Fig. 3. Circular dichroism spectra of the cuproxidases *Pha*MOx (blue), CueO (green) and *Tth*-MCO (red). A: CD spectra in the far-UV region induced mainly by the secondary structures. B: CD spectra in the near-UV region induced mainly by aromatic side chains (250–300 nm) and by copper ions (>300 nm).

physiological form available in the cell. Accordingly, full holoenzymes were prepared by adding excess Cu(I) in the form of an acetonitrile delivery complex $[Cu(I)(MeCN)_4]^+$. Cu(I) ions added were incorporated into the copper centers and the excess was then a substrate of the enzyme, which was rapidly oxidized. This excess was removed by gel filtration and the holoenzymes were used for all subsequent experiments unless otherwise stated.

Copper content of the purified enzymes was determined by the 2,2′-biquinoline method [32] before and after the treatment described above. Increase in copper content was observed for all MCOs (Table 3). After Cu(I) loading, one should expect a total of 4 copper atoms per holoenzyme molecule under aerobic conditions. Deviations from this stoichiometry in Table 3 arises mainly from

Table 3
Copper binding by the homologous multicopper oxidases and by *Pha*MOx mutants (molar ratios).

	Purified enzymes	+ excess Cu(I) in aerobic conditions		+ excess Cu(I) in anaerobic conditions		Extra Cu(I) binding in anaerobic conditions
	Cu total	Experimental Cu total	Normalized Cu total	Cu(I)	Cu total	
Tth-MCO	1.5 ± 0.1	5.6 ± 0.1	4.0 ± 0.1	5.4 ± 0.1	5.4 ± 0.1	1.4 ± 0.1
CueO	7.6 ± 0.2	8.6 ± 0.1	4.0 ± 0.1	7.5 ± 0.1	7.4 ± 0.1	3.5 ± 0.1
*Pha*MOx	3.7 ± 0.2	5.1 ± 0.1	4.0 ± 0.1	13.2 ± 0.1	13.0 ± 0.1	9.2 ± 0.2
*Pha*MOx Δ1	3.5 ± 0.1	5.3 ± 0.1	4.0 ± 0.1	12.5 ± 0.2	12.5 ± 0.2	8.5 ± 0.2
*Pha*MOx Δ3	3.1 ± 0.1	4.8 ± 0.1	4.0 ± 0.1	5.7 ± 0.1	5.7 ± 0.1	1.7 ± 0.2
*Pha*MOx Δ23	3.4 ± 0.3	4.7 ± 0.1	4.0 ± 0.1	7.4 ± 0.1	7.4 ± 0.1	3.4 ± 0.1

cumulative errors on protein concentration. Accordingly, the copper content of holoenzymes was normalized to 4 Cu atoms per enzyme molecule for further calculations (see below).

To analyze the Cu(I) binding capacity of the homologous blue oxidases, the main issue was to resolve the instability of Cu(I) ion due to its fast oxidation to Cu(II) either directly by O_2 or by the enzyme. We have developed a new methodology for copper loading and for the determination of copper content using an excess of reductant and under strict N_2 atmosphere in order to block the catalytic turnover and oxidation of Cu(I) to Cu(II) (see *2.4.* for details). As shown in Table 3, the Cu(I) content of holoenzymes under anaerobic conditions was identical to the total copper content. This demonstrates that all copper atoms bound to the enzyme and quantified have been maintained in the cuprous state along the manipulation. Accordingly, subtracting the 4 copper atoms belonging to the active site from the copper content under anaerobic conditions provided the number of extra Cu(I) ions bound to the enzymes: *Tth*-MCO binds only ~1 extra Cu(I), ~3 extra Cu(I) ions are found for CueO and *Pha*MOx binds ~9 extra Cu(I) ions. It is worth mentioning that the result obtained for CueO is in excellent agreement with the 3 Cu(I) ions bound to the Met-rich insert in its high resolution crystal structure [14,15] and tends to validate our approach. Furthermore, the number of extra Cu(I) appears to be almost correlated with the length of the Met-rich loops and to the number of potential Cu(I) ligands (Table 2). The latter hypothesis was addressed by mutagenesis of the psychrophilic *Pha*MOx because of its high Cu(I) binding capacity and specific loop properties as detailed below.

3.6. Design of PhaMOx mutants

Based on sequence alignment comparison (Fig. S4) and on the crystal structures of CueO [14] and *Tth*-MCO [20], we have identified regions at the surface of *Pha*MOx near the T1 site potentially involved in its cuproxidase function. These regions are predicted to be disordered by algorithms such as PSIPRED [33]. In order to explore the role of these regions in *Pha*MOx, three different mutants have been constructed (Fig. 4).

(i) The mutant Δ1 in which a putative surface loop close to the T1 site and formed by residues 181 to 212 (native form numbering, 217–248 in the precursor) has been deleted. This loop is much longer as compared to CueO and *Tth*-MCO and is inserted at location 2 of other cuproxidases. Although it does not display the canonical Met and His-rich signature, the proximity to the T1 site might confer a specific function to this loop.
(ii) The mutant Δ3 in which the Met-rich region has been deleted (residues 347 to 394 deleted, 383–430 in the precursor), but keeping the outer sCu consensus sequence intact with Met340 and Asp342 as candidates for sCu coordination by the outer part of the binding site.
(iii) The mutant Δ23 in which both the entire Met-rich region and the outer sCu consensus sequence MRDMMG were removed (residues 340 to 394, 376–430 in the precursor). Both latter mutants could validate our consensus sequence for the sCu site.

3.7. Characterization of PhaMOx mutants

The three mutant enzymes were produced and purified according to the wild-type procedure and the copper content was similar both at the end of the purification and after treatment with the acetonitrile delivery complex $[Cu(I)(MeCN)_4]^+$ to obtain full holoenzymes (Table 3). The CD spectra in the far UV region of the mutants as compared to *Pha*MOx (Fig. 5A) indicated that no significant changes in secondary structures have occurred upon deletion of the loops, in agreement with their predicted disordered conformation. Spectra in the near UV region (Fig. 5B) also indicated that the tertiary structures and the copper centers remained unaffected by these loop deletions. Structural stability analyzed by DSC was performed on apoenzymes because copper release during thermal unfolding of the holoenzymes induced aggregation and precluded reliable thermogram records. The normalized DSC thermograms (Fig. 6A) and stability parameters (Table 4) of the mutants were similar to the parent *Pha*MOx, demonstrating that the Met-rich region has no influence on the cuproxidase stability.

By contrast, the effect of Cu(II) concentration on the laccase-like activity of the mutants with 2,6-dimethoxyphenol as substrate revealed distinct features (Fig. 6B and Table 4). Deletion of both the postulated outer part of the sCu site and of the Met-rich loop in mutant Δ23 resulted in 93% loss of activity, highlighting the importance of this region for phenol-oxidase activity, with however an improved apparent affinity for Cu(II). The severe activity decrease of mutant Δ23 arises from deletion of the MRDMMG sequence as evidenced by mutant Δ3. Indeed, the latter contains this sCu consensus sequence and retains 76% of the wild-type *Pha*MOx activity with similar apparent affinity for Cu(II). This also strongly suggests that the outer sCu consensus sequence in the Met-rich region, determined from our multiple sequence alignment, actually corresponds to the outer part of the sCu binding site. Unexpectedly, mutant Δ1 only retained 20% of activity with almost unaffected apparent affinity for Cu(II).

The Cu(I) binding ability of the mutants was assayed under anaerobic conditions (Table 3). The mutant Δ1 displayed an almost unaffected Cu(I) binding capacity as compared with *Pha*MOx. This shows that the loop 181–212 specific to *Pha*MOx is not involved in Cu(I) chelation. This mutant can also be regarded as a positive control, as deletion of the loop devoid of the Met-rich signature does not affect the Cu(I) binding ability. In contrast, removal of the Met-rich region decreases the number of extra Cu(I) bound from ~9 in *Pha*MOx to ~2 or ~3 in Δ3 and Δ23, respectively. The residual Cu(I) bound to the mutants can be regarded as non-specific binding

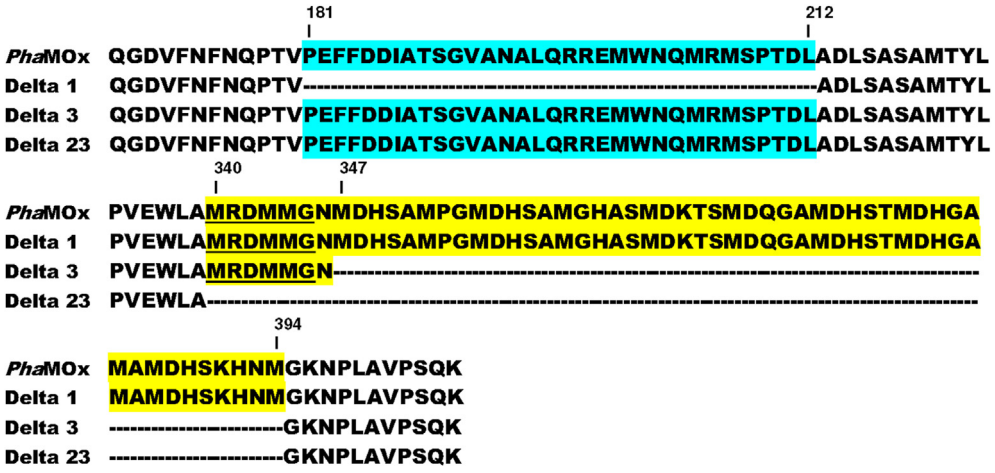

Fig. 4. Partial amino acid sequences of *Pha*MOx and of its deletion mutants. Numbering refers to the *Pha*MOx native form. The consensus sequence of the outer part of the sCu site is underlined.

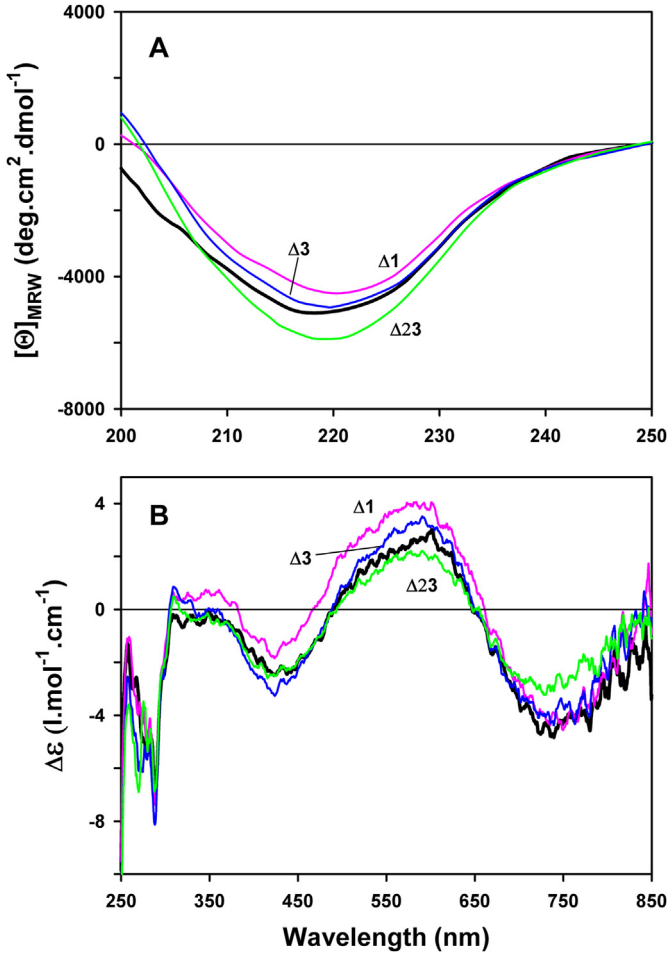

Fig. 5. Circular dichroism spectra of *Pha*MOx and of its mutants. A: CD spectra in the far-UV region (*Pha*MOx spectrum in heavy black trace). B: CD spectra in the near-UV region (*Pha*MOx spectrum in heavy black trace).

or they might also reflect distinct Cu(I) binding ability of the core enzyme.

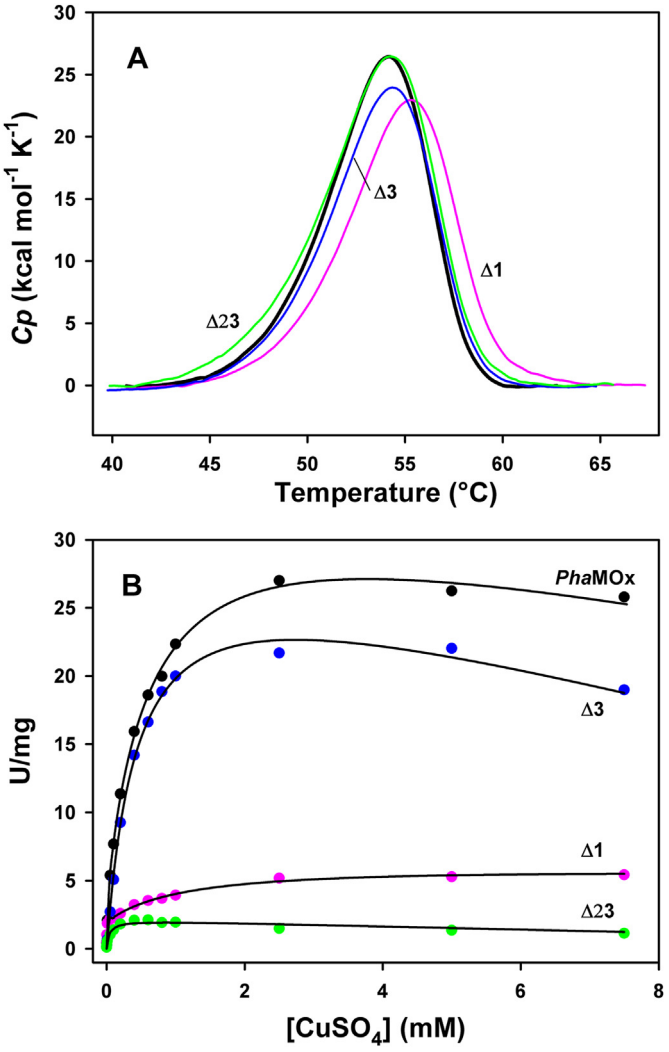

Fig. 6. Stability and laccase-like activity of *Pha*MOx and of its mutants. A: Differential scanning calorimetry of the apoenzymes. Heavy black line: thermogram of the wild-type *Pha*MOx. T_m was measured at the top of the transition and ΔH_{cal} was calculated as the area under the transition. B: Cu(II) dependence of laccase-like activity at 25 °C (1 U = 1 μmole of 2,6-dimethoxyphenol oxidized per min).

Table 4
Stability and laccase-like activity of *Pha*MOx and of its mutants.

	DSC		Laccase-like activity	
	Tm °C	ΔH_{cal} kcal mol^{-1}	V_{max} U mg^{-1}	$K_{d\ app}$ μM
*Pha*MOx	54.2	178	28.8 ± 0.9	334 ± 16
*Pha*MOx Δ 1	55.3	160	5.6 ± 0.2	259 ± 13
*Pha*MOx Δ 3	54.3	158	22.0 ± 0.7	271 ± 13
*Pha*MOx Δ 23	54.1	180	2.1 ± 0.1	53 ± 3

SD are ±0.1 °C on *Tm* and ±5% on ΔH_{cal}.

4. Discussion

Methionin-rich regions are frequently associated with proteins involved in copper trafficking, management and homeostasis. Indeed, the thioether group of methionine has been shown to play a major role in the bioinorganic chemistry of Cu(I) ions [34]. For instance, a simple peptide containing a MXXMXXM motif is sufficient to bind Cu(I) ions with very high affinity [35]. Methionine motifs for copper binding are resistant to oxidation and therefore are mainly found in cell compartments exposed to oxidative environment, in contrast with the oxidation-prone cysteine motifs which are mainly found in the reducing intracellular environment. MCOs from bacterial species which possess Met-rich regions can only be found in the periplasm of prokaryotes where their physiological role is the defense of this important cell compartment against toxic cuprous ions. In CueO, the low coordination number, solvent exposure, and disorder of the methionine-rich binding sites make them suitable for transient copper binding and substrate procurement [14]. Here we have shown that location, size and sequence of these Met-rich inserts are highly variable in bacterial cuproxidases and that they bind specifically Cu(I) with a stoichiometry related to their size and composition in three investigated blue oxidases. It is worth mentioning that Cu(I) binding has been only demonstrated for CueO on the basis of its high resolution crystal structure [14]. Here we provide a new method for cuprous ion binding determination in reducing solution and oxygen-less atmosphere, which can be applied to any potential cuproxidase.

In sharp contrast with most functional motifs which have a well-defined position in protein structures, the Met-rich inserts in bacterial MCOs were found at locations corresponding to six different solvent exposed loops of the cuproxidase CueO (Fig. 2). However, these loops share a close spatial proximity with the strictly conserved blue T1 site which bind the first catalytic copper. It should be noted that all insertions of a Met-rich region (with only one exception at region 5) occur in the cupredoxin domain 2 and as N- or C-terminal tails (Fig. 1). Domain 2 is the longest in the sequence but does not carry any of the active site copper chelating residues. The T1 site is located in the cupredoxin domain 3 and the trinuclear copper binding site is formed at the interface of domains 1 and 3. Accordingly, one can suggest that both cupredoxin domains 1 and 3 are not (or less) amenable to Met-rich loop insertion, whereas domain 2 possesses sufficient structural plasticity to accommodate such insertions.

In the 3 cuproxidases investigated here, these Met-rich regions display a conserved N-terminal M(X)DM(X)G motif (Fig. S4) in which both Met and Asp residues form the outer part of the sCu site in CueO [27]. The involvement of this conserved motif in the sCu site of other bacterial cuproxidases is supported by the Δ23 mutant of *Pha*MOx: deletion of this motif results in a drastic reduction of phenol oxidase activity, which requires Cu(II) binding to this site (Fig. 6B and Table 4). In addition, the 3 blue oxidases possess strongly conserved Asp and Met residues immediately upstream from the strictly conserved histidines of the T1 site (Fig. S4) and forming the buried inner part of the sCu site in CueO [27]. In most cases, the sequence of the outer part was hardly detectable within the primary structures of other cuproxidases. However, the occurrence of M and/or D and/or H immediately upstream of the conserved copper-binding histidines is a novel criterion allowing to distinguish cuproxidases from other MCOs (Figs. S1 and S3). Furthermore, our newly developed method for cuprous ion binding determination will allow to experimentally check this criterion. Altogether, the occurrence of the Met-rich inserts and of both sCu motifs support the possible early events in Cu(I) oxidation proposed for CueO and their generalization in bacterial cuproxidases: the Met-rich regions chelate Cu(I) in the periplasm and are dedicated to feed the sCu site. They provide a first step of electron transfer to the catalytic copper T1 and to the trinuclear center [14,15]. Cuproxidases can then be regarded as molecular octopus with a beak (the sCu site) and tentacles (the Met-rich Cu(I) binding region).

The deletion mutants of *Pha*MOx also provide additional structural and functional information. None of these deletions induce major changes in the CD spectra (Fig. 5) nor in the stability parameters of the mutants (Fig. 6A, Table 4). This indicates that the deleted regions are not closely packed on the core enzyme, but rather are disordered loops as also predicted by PSIPRED. The slight increase of stability (positive shift of ~1 °C in T_m) observed for the mutant Δ1, suggests that this surface loop (devoid of the Met-rich signature) exerts a constraint on the core enzyme, which was relieved upon deletion. This loop is not involved in Cu(I) binding (Table 3) but its deletion results in an 80% loss of laccase-like activity. This indicates that the loop 181–212 specific to *Pha*MOx and not related to the Met-rich region is involved in the phenol-oxidase activity. More importantly, the severe loss of Cu(I) ions bound to mutant Δ3 and Δ23 demonstrates that the Met-rich insert is specifically designed to coordinate several Cu(I) ions.

The physiological relevance of length variability in Met-rich inserts remains unclear. Indeed, long insert sequences potentially binding more Cu(I) are found in bacterium not exposed to high copper concentrations such as *P. haloplanktis* isolated from pristine Antarctic sea ice. Conversely, short insert sequences are noted in thermophiles thriving in metal-rich effluents from hot springs, although this could be possibly related to loop length decreases in thermophilic proteins in order to improve their stability. Nevertheless, variability in location, length and sequence of Met-rich inserts suggests evolutionary trend and selection for the acquirement of copper-binding residues in surface loops close to the blue T1 site.

Finally, we have shown that the three cuproxidases can be produced intracellularly in a functional but almost Cu-depleted form in the absence of copper in the culture medium and that the enzymes can be activated by an exogenous Cu(I) supply. This has at least two physiological consequences. Induction of cuproxidase synthesis is thought to be mediated by the appearance of Cu(I) in the cytoplasm. Accordingly, following cuproxidase synthesis, its copper loading process can already contribute to lower the level of toxic intracellular Cu(I), although CueO from *E. coli* was found to be exported as an apoenzyme [24]. Furthermore, if the induction mechanism is not tightly regulated, a basal level of Cu-depleted cuproxidase can be synthesized and translocated in the periplasm by the Tat secretion apparatus. This pool of poorly active cuproxidase might be regarded as a first line defense, waiting for Cu(I) loading and full oxidase activity.

Authors' contribution

F.R. and A.G. performed the experiments. F.R. and G.F. designed the study and wrote the manuscript. All authors reviewed and approved the final version of the manuscript.

Data availability statement

The data underlying this article are available in the article and in its online Supplementary data.

Declaration of competing interest

The authors declare no conflict of interest.

Acknowledgements

We thanks Dr. Kentaro Miyazaki for providing the *Tth*-MCO expression plasmid. This work was supported by the F.R.S-FNRS, Belgium (Fonds de la Recherche Fondamentale et Collective, contract numbers 2.4535.08, 2.4523.11 and U.N009.13 to G.F.). F.R. and A.G. were FRIA research fellows during this work.

Appendix A. Supplementary data

Supplementary data to this article can be found online at https://doi.org/10.1016/j.biochi.2021.12.015.

References

[1] R.R. Crichton, J.L. Pierre, Old iron, young copper: from Mars to Venus, Biometals 14 (2001) 99–112. http://www.ncbi.nlm.nih.gov/pubmed/11508852.
[2] D. Magnani, M. Solioz, How bacteria handle copper, in: D.H. Nies, S. Silver (Eds.), Microbiology of Heavy Metals, Springer, Berlin, 2007, pp. 259–285.
[3] J.H. Kaplan, S. Lutsenko, Copper transport in mammalian cells: special care for a metal with special needs, J. Biol. Chem. 284 (2009) 25461–25465. http://www.ncbi.nlm.nih.gov/pubmed/19602511.
[4] B.E. Kim, T. Nevitt, D.J. Thiele, Mechanisms for copper acquisition, distribution and regulation, Nat. Chem. Biol. 4 (2008) 176–185. http://www.ncbi.nlm.nih.gov/pubmed/18277979.
[5] S. Tottey, K.J. Waldron, S.J. Firbank, B. Reale, C. Bessant, K. Sato, T.R. Cheek, J. Gray, M.J. Banfield, C. Dennison, N.J. Robinson, Protein-folding location can regulate manganese-binding versus copper- or zinc-binding, Nature 455 (2008) 1138–1142. http://www.ncbi.nlm.nih.gov/pubmed/18948958.
[6] G. Grass, C. Rensing, Genes involved in copper homeostasis in *Escherichia coli*, J. Bacteriol. 183 (2001) 2145–2147. http://www.ncbi.nlm.nih.gov/pubmed/11222619.
[7] C. Rensing, G. Grass, *Escherichia coli* mechanisms of copper homeostasis in a changing environment, FEMS Microbiol. Rev. 27 (2003) 197–213. http://www.ncbi.nlm.nih.gov/pubmed/12829268.
[8] E.I. Solomon, A.J. Augustine, J. Yoon, O_2 reduction to H_2O by the multicopper oxidases, Dalton Trans. 30 (2008) 3921–3932. http://www.ncbi.nlm.nih.gov/pubmed/18648693.
[9] L. Quintanar, C. Stoj, A.B. Taylor, P.J. Hart, D.J. Kosman, E.I. Solomon, Shall we dance? How a multicopper oxidase chooses its electron transfer partner, Acc. Chem. Res. 40 (2007) 445–452. http://www.ncbi.nlm.nih.gov/pubmed/17425282.
[10] D.J. Kosman, Multicopper oxidases: a workshop on copper coordination chemistry, electron transfer, and metallophysiology, J. Biol. Inorg. Chem. 15 (2010) 15–28. http://www.ncbi.nlm.nih.gov/pubmed/19816718.
[11] D. Sirim, F. Wagner, L. Wang, R.D. Schmid, J. Pleiss, The Laccase Engineering Database: a Classification and Analysis System for Laccases and Related Multicopper Oxidases, Database, Oxford), 2011 (2011) bar006, http://www.ncbi.nlm.nih.gov/pubmed/21498547.
[12] C.S. Stoj, A.J. Augustine, E.I. Solomon, D.J. Kosman, Structure-function analysis of the cuprous oxidase activity in Fet3p from *Saccharomyces cerevisiae*, J. Biol. Chem. 282 (2007) 7862–7868. http://www.ncbi.nlm.nih.gov/pubmed/17220296.
[13] K.Y. Djoko, L.X. Chong, A.G. Wedd, Z. Xiao, Reaction mechanisms of the multicopper oxidase CueO from *Escherichia coli* support its functional role as a cuprous oxidase, J. Am. Chem. Soc. 132 (2010) 2005–2015. http://www.ncbi.nlm.nih.gov/pubmed/20088522.
[14] S.K. Singh, S.A. Roberts, S.F. McDevitt, A. Weichsel, G.F. Wildner, G.B. Grass, C. Rensing, W.R. Montfort, Crystal structures of multicopper oxidase CueO bound to copper(I) and silver(I): functional role of a methionine-rich sequence, J. Biol. Chem. 286 (2011) 37849–37857. http://www.ncbi.nlm.nih.gov/pubmed/21903583.
[15] L. Cortes, A.G. Wedd, Z. Xiao, The functional roles of the three copper sites associated with the methionine-rich insert in the multicopper oxidase CueO from *E. coli*, Metallomics 7 (2015) 776–785. http://www.ncbi.nlm.nih.gov/pubmed/25679350.
[16] A.T. Fernandes, C.M. Soares, M.M. Pereira, R. Huber, G. Grass, L.O. Martins, A robust metallo-oxidase from the hyperthermophilic bacterium *Aquifex aeolicus*, FEBS J. 274 (2007) 2683–2694. http://www.ncbi.nlm.nih.gov/pubmed/17451433.
[17] H. Sakuraba, K. Koga, K. Yoneda, Y. Kashima, T. Ohshima, Structure of a multicopper oxidase from the hyperthermophilic archaeon *Pyrobaculum aerophilum*, Acta Crystallogr. Sect. F Struct. Biol. Cryst. Commun. 67 (2011) 753–757. http://www.ncbi.nlm.nih.gov/pubmed/21795787.
[18] S.A. Roberts, A. Weichsel, G. Grass, K. Thakali, J.T. Hazzard, G. Tollin, C. Rensing, W.R. Montfort, Crystal structure and electron transfer kinetics of CueO, a multicopper oxidase required for copper homeostasis in *Escherichia coli*, Proc. Natl. Acad. Sci. U.S.A. 99 (2002) 2766–2771. http://www.ncbi.nlm.nih.gov/pubmed/11867755.
[19] K. Miyazaki, A hyperthermophilic laccase from *Thermus thermophilus* HB27, Extremophiles 9 (2005) 415–425. http://www.ncbi.nlm.nih.gov/pubmed/15999224.
[20] M. Bello, B. Valderrama, H. Serrano-Posada, E. Rudino-Pinera, Molecular dynamics of a thermostable multicopper oxidase from *Thermus thermophilus* HB27: structural differences between the apo and holo forms, PLoS One 7 (2012), e40700. http://www.ncbi.nlm.nih.gov/pubmed/22808237.
[21] C. Medigue, E. Krin, G. Pascal, V. Barbe, A. Bernsel, P.N. Bertin, F. Cheung, S. Cruveiller, S. D'Amico, A. Duilio, G. Fang, G. Feller, C. Ho, S. Mangenot, G. Marino, J. Nilsson, E. Parrilli, E.P. Rocha, Z. Rouy, A. Sekowska, M.L. Tutino, D. Vallenet, G. von Heijne, A. Danchin, Coping with cold: the genome of the versatile marine Antarctica bacterium *Pseudoalteromonas haloplanktis* TAC125, Genome Res. 15 (2005) 1325–1335. http://www.ncbi.nlm.nih.gov/pubmed/16169927.
[22] F. Roulling, A. Godin, A. Cipolla, T. Collins, K. Miyazaki, G. Feller, Activity-stability relationships revisited in blue oxidases catalyzing electron transfer at extreme temperatures, Extremophiles (2016) 621–629. http://www.ncbi.nlm.nih.gov/pubmed/27315165.
[23] T. Palmer, B.C. Berks, The twin-arginine translocation (Tat) protein export pathway, Nat. Rev. Microbiol. 10 (2012) 483–496. http://www.ncbi.nlm.nih.gov/pubmed/22683878.
[24] P. Stolle, B. Hou, T. Bruser, The Tat substrate CueO is transported in an incomplete folding state, J. Biol. Chem. 291 (2016) 13520–13528. http://www.ncbi.nlm.nih.gov/pubmed/27129241.
[25] C.S. Silva, P. Durao, A. Fillat, P.F. Lindley, L.O. Martins, I. Bento, Crystal structure of the multicopper oxidase from the pathogenic bacterium *Campylobacter jejuni* CGUG11284: characterization of a metallo-oxidase, Metallomics 4 (2012) 37–47. http://www.ncbi.nlm.nih.gov/pubmed/22127520.
[26] T. Classen, J. Pietruszka, S.M. Schuback, A new multicopper oxidase from Gram-positive bacterium *Rhodococcus erythropolis* with activity modulating methionine rich tail, Protein Expr. Purif 89 (2013) 97–108. http://www.ncbi.nlm.nih.gov/pubmed/23485678.
[27] S.A. Roberts, G.F. Wildner, G. Grass, A. Weichsel, A. Ambrus, C. Rensing, W.R. Montfort, A labile regulatory copper ion lies near the T1 copper site in the multicopper oxidase CueO, J. Biol. Chem. 278 (2003) 31958–31963. http://www.ncbi.nlm.nih.gov/pubmed/12794077.
[28] G. Feller, Protein stability and enzyme activity at extreme biological temperatures, J. Phys. Condens. Matter 22 (2010), 323101. https://pubmed.ncbi.nlm.nih.gov/21386475.
[29] R. Papa, E. Parrilli, G. Sannia, Engineered marine Antarctic bacterium *Pseudoalteromonas haloplanktis* TAC125: a promising micro-organism for the bioremediation of aromatic compounds, J. Appl. Microbiol. 106 (2009) 49–56. http://www.ncbi.nlm.nih.gov/pubmed/19120609.
[30] T.N. Petersen, S. Brunak, G. von Heijne, H. Nielsen, SignalP 4.0: discriminating signal peptides from transmembrane regions, Nat. Methods 8 (2011) 785–786. http://www.ncbi.nlm.nih.gov/pubmed/21959131.
[31] G. Musci, S. Di Marco, G.C. Bellenchi, L. Calabrese, Reconstitution of ceruloplasmin by the Cu(I)-glutathione complex. Evidence for a role of Mg^{2+} and ATP, J. Biol. Chem. 271 (1996) 1972–1978. http://www.ncbi.nlm.nih.gov/pubmed/8567646.
[32] G. Felsenfeld, The determination of cuprous ion in copper proteins, Arch. Biochem. Biophys. 87 (1960) 247–251. http://www.ncbi.nlm.nih.gov/pubmed/13822131.
[33] D.W. Buchan, F. Minneci, T.C. Nugent, K. Bryson, D.T. Jones, Scalable web services for the PSIPRED protein analysis workbench, Nucleic Acids Res. 41 (2013) W349–W357. http://www.ncbi.nlm.nih.gov/pubmed/23748958.
[34] A.V. Davis, T.V. O'Halloran, A place for thioether chemistry in cellular copper ion recognition and trafficking, Nat. Chem. Biol. 4 (2008) 148–151. http://www.ncbi.nlm.nih.gov/pubmed/18277969.
[35] J. Jiang, I.A. Nadas, M.A. Kim, K.J. Franz, A Mets motif peptide found in copper transport proteins selectively binds Cu(I) with methionine-only coordination, Inorg. Chem. 44 (2005) 9787–9794. http://www.ncbi.nlm.nih.gov/pubmed/16363848.
[36] C. Kim, W.W. Lorenz, J.T. Hoopes, J.F. Dean, Oxidation of phenolate siderophores by the multicopper oxidase encoded by the *Escherichia coli yacK* gene, J. Bacteriol. 183 (2001) 4866–4875. http://www.ncbi.nlm.nih.gov/pubmed/11466290.